
Learning to Infer Graphics Programs from Hand-Drawn Images

Anonymous Author(s)

Affiliation

Address

email

Abstract

1 We introduce a model that learns to convert simple hand drawings into graphics
2 programs written in a subset of \LaTeX . The model combines techniques from deep
3 learning and program synthesis. We learn a convolutional neural network that
4 proposes plausible drawing primitives that explain an image. This set of drawing
5 primitives is like an execution trace for a graphics program. From this trace we use
6 program synthesis techniques to recover a graphics program with constructs like
7 variable bindings, iterative loops, or simple kinds of conditionals. With a graphics
8 program in hand, we can correct errors made by the deep network, cluster drawings
9 by use of similar high-level geometric structures, and extrapolate drawings. Taken
10 together these results are a step towards agents that induce useful, human-readable
11 programs from perceptual input.

1 Introduction

13 How can an agent convert noisy, high-dimensional perceptual input to a symbolic, abstract object, such
14 as a computer program? Here we consider this problem within a graphics program synthesis domain.
15 We develop an approach for converting natural images, such as hand drawings, into executable source
16 code for drawing the original image. The graphics programs in our domain draw simple figures like
17 those found in machine learning papers (see Figure 1).

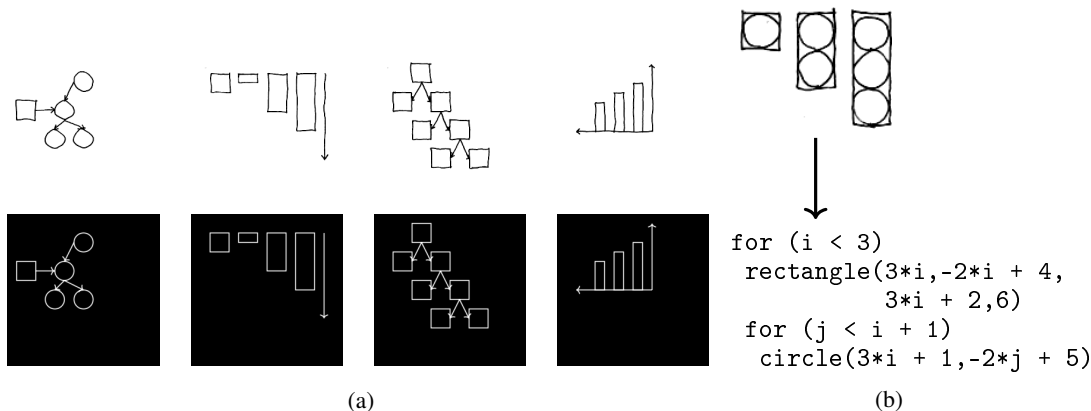


Figure 1: (a): Model learns to convert hand drawings (top) into \LaTeX (bottom). (b) Synthesizes high-level *graphics program* from hand drawing.

High dimensional perceptual input may seem ill matched to the abstract semantics of a programming language. But programs with constructs such as recursion or iteration produce a simpler *execution trace* of primitive actions; for our domain, the primitive actions are drawing commands. Our hypothesis is that the execution trace of the program is better aligned with the perceptual input, and that the trace can act as a kind of bridge between perception and programs. We test this hypothesis by developing a model that learns to map from an image to the execution trace of the graphics program that drew it. With the execution trace in hand, we can bring to bear techniques from the program synthesis community to recover the latent graphics program. This family of techniques, called *constraint-based program synthesis* [1], work by modeling a set of possible programs inside of a constraint solver, such as a SAT or SMT solver [2]. These techniques excel at uncovering high-level symbolic structure, but are not well equipped to deal with real-valued perceptual inputs.

We develop a hybrid architecture for inferring graphics programs. Our approach uses a deep neural network infer an execution trace from an image; this network recovers primitive drawing operations such as lines, circles, or arrows, along with their parameters. For added robustness, we use the deep network as a proposal distribution for a stochastic search over execution traces. Section 3 describes this first stage of the architecture where we infer drawing commands from images, and explains how we handle noisy hand drawings. Finally, we use program synthesis techniques to recover the program from its trace. The program synthesizer discovers constructs such as loops and geometric operations such as reflections and affine transformations. Section 4 describes how the architecture synthesizes programs from execution traces, and how those programs are used for correcting errors made by the deep network, measuring similarity between hand drawings, and extrapolating figures.

2 Related work

Our work bears resemblance to the Attend-Infer-Repeat (AIR) system, which learns to decompose an image into its constituent objects [3]. AIR learns an iterative inference scheme which infers objects one by one and also decides when to stop inference; this is similar to our approach’s first stage, which parses images into program execution traces. Our approach further produces interpretable, symbolic programs which generate those execution traces. The two approaches also differ in their architectures and training regimes: AIR learns a recurrent auto-encoding model via variational inference, whereas our parsing stage learns an autoregressive-style model from randomly-generated (execution trace, image) pairs. Finally, while AIR was evaluated on multi-MNIST images and synthetic 3D scenes, we focus on parsing and interpreting hand-drawn sketches.

Our image-to-execution-trace parsing architecture builds on prior work on controlling procedural graphics programs [4]. Given a program which generates random 2D recursive structures such as vines, that system learns a structurally-identical “guide program” whose output can be directed, via neural networks, to resemble a given target image. We adapt this method to a different visual domain (figures composed of multiple objects), using a broad prior over possible scenes as the initial program and viewing the execution trace through the guide program as a symbolic parse of the target image. We then show how to synthesize higher-level programs from these execution traces.

In the computer graphics literature, there have been other systems which convert sketches into procedural representations. One uses a convolutional network to match a sketch to the output of a parametric 3D modeling system [5]. Another uses convolutional networks to support sketch-based instantiation of procedural primitives within an interactive architectural modeling system [6]. Both systems focus on inferring fixed-dimensional parameter vectors. In contrast, we seek to automatically infer a structured, programmatic representation of a sketch which captures higher-level visual patterns.

Prior work has also applied sketch-based program synthesis to authoring graphics programs. In particular, Sketch-n-Sketch presents a bi-directional editing system in which direct manipulations to a program’s output automatically propagate to the program source code [7]. We see this work as complementary to our own: programs produced by our method could be provided to a Sketch-n-Sketch-like system as a starting point for further editing.

The CogSketch [8] system also aims to have a high-level understanding of hand-drawn figures. Their primary goal is cognitive modeling (eg, they apply their system to solving IQ-test style visual reasoning problems), whereas we are interested in building an automated AI application (eg, in our system the user need not annotate which strokes correspond to which shapes; our neural network produces something equivalent to the annotations). A key similarity however is that both CogSketch

<code>circle(x, y)</code>	Circle at (x, y)
<code>rectangle(x_1, y_1, x_2, y_2)</code>	Rectangle with corners at (x_1, y_1) & (x_2, y_2)
<code>line(x_1, y_1, x_2, y_2, arrow $\in \{0, 1\}$, dashed $\in \{0, 1\}$)</code>	Line from (x_1, y_1) to (x_2, y_2) , optionally with an arrow and/or dashed
<code>STOP</code>	Finishes execution trace inference

Table 1: The deep network in (2) predicts drawing commands, shown above.

and our system have as a goal to make it easier to produce nice-looking figures. Unsupervised Program Synthesis [9] is a related framework which was also applied to geometric reasoning problems. The goals of [9] were cognitive modeling, and they applied their technique to synthetic scenes used in human behavioral studies.

3 Neural architecture for inferring drawing execution traces

We developed a deep network architecture for efficiently inferring a execution trace, T , from an image, I . Our model constructs the trace one drawing command at a time. When predicting the next drawing command, the network takes as input the target image I as well as the rendered output of previous drawing commands. Intuitively, the network looks at the image it wants to explain, as well as what it has already drawn. It then decides either to stop drawing or proposes another drawing command to add to the execution trace; if it decides to continue drawing, the predicted primitive is rendered to its “canvas” and the process repeats.

Figure 2 illustrates this architecture. We first pass a 256×256 target image and a rendering of the trace so far (encoded as a two-channel image) to a convolutional network. Given the features extracted by the convnet, a multilayer perceptron then predicts a distribution over the next drawing command to add to the trace. We predict the drawing command token-by-token, conditioning each token both on the image features and on the previously generated tokens. For example, the network first decides to emit the `circle` token conditioned on the image features, then it emits the x coordinate of the circle conditioned on the image features and the `circle` token, and finally it predicts the y coordinate of the circle conditioned on the image features, the `circle` token, and the x coordinate. See supplement for the full details of the architecture, which we implemented in Tensorflow [10].

The distribution over the next drawing command factorizes as:

$$\mathbb{P}_\theta[t_1 t_2 \cdots t_K | I, T] = \prod_{k=1}^K \mathbb{P}_\theta[t_k | f_\theta(I, \text{render}(T)), \{t_j\}_{j=1}^{k-1}] \quad (1)$$

where $t_1 t_2 \cdots t_K$ are the tokens in the drawing command, I is the target image, T is an execution trace, θ are the parameters of the neural network, and $f_\theta(\cdot, \cdot)$ is the image feature extractor (convolutional network). The distribution over execution traces factorizes as:

$$\mathbb{P}_\theta[T | I] = \prod_{n=1}^{|T|} \mathbb{P}_\theta[T_n | I, T_{1:(n-1)}] \times \mathbb{P}_\theta[\text{STOP} | I, T] \quad (2)$$

where $|T|$ is the length of execution trace T , and the subscripts on T index drawing commands within the trace, and the `STOP` token is emitted by the network to signal that the execution trace explains the image.

We train the network by sampling execution traces T and target images I for randomly generated scenes and maximizing (2) with respect to θ by gradient ascent. Training does not require back-propagation across the entire sequence of drawing commands: drawing to the canvas ‘blocks’ the gradients, effectively offloading memory to an external visual store. In a sense, this model is like an autoregressive variant of AIR [3] without attention.

We trained the network on 10^5 scenes, which takes a little less than a day on a Nvidia TitanX GPU.

This network suffices to “derender” synthetic images like those shown in Figure 3. We can perform a beam search decoding to recover what the network thinks is the most likely execution trace for images like these, recovering traces maximizing $\mathbb{P}_\theta[T | I]$. But, if the network makes a mistake (predicts an

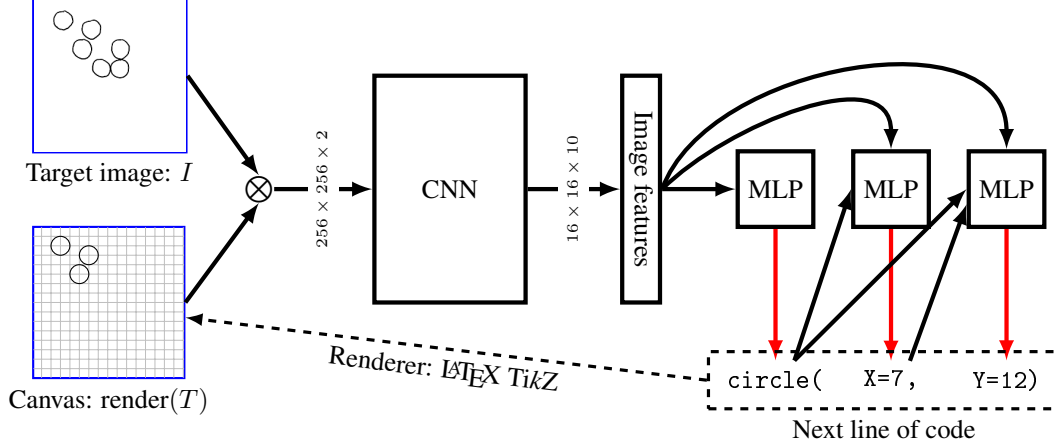


Figure 2: Our neural architecture for inferring the execution trace of a graphics program from its output. **Blue**: network inputs. **Black**: network operations. **Red**: samples from a multinomial. Typewriter font: network outputs. Renders snapped to a 16×16 grid, illustrated in gray.

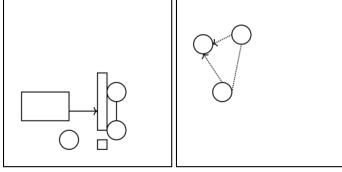


Figure 3: Network is trained to infer execution traces for randomly generated scenes like the two shown above. See supplement for details of the training data generation.

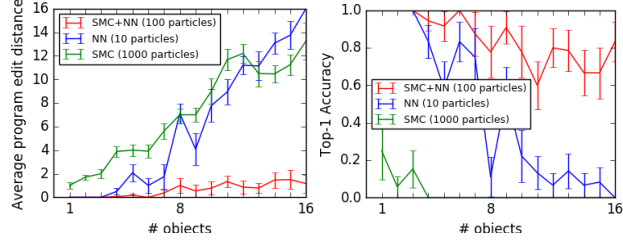


Figure 4: Using the model to parse latex output. The model is trained on diagrams with up to 8 objects. As shown above it generalizes to scenes with many more objects. Neither the stochastic search nor the neural network are sufficient on their own. # particles varies by model: we compare the models *with equal runtime* (≈ 1 sec/object)

incorrect line of code), it has no way of recovering from the error. In order to derender an image with n objects, it must correctly predict n drawing commands – so its probability of success will decrease exponentially in n , assuming it has any nonzero chance of making a mistake. For added robustness as n becomes large, we treat the neural network outputs as proposals for a Sequential Monte Carlo (SMC) sampling scheme [11]. For the SMC sampler, we use pixel-wise distance as a surrogate for a likelihood function. The SMC sampler is designed to produce samples from the distribution $\propto L(I|\text{render}(T))\mathbb{P}_\theta[T|I]$, where $L(\cdot|\cdot) : \text{image}^2 \rightarrow \mathcal{R}$ uses the distance between two images as a proxy for a likelihood.

Figure 4 compares the neural network with SMC against the neural network by itself or SMC by itself. Only the combination of the two passes a critical test of generalization: when trained on images with ≤ 8 objects, it successfully parses scenes with many more objects than the training data.

3.1 Generalizing to hand drawings

A practical application of our neural network is the automatic conversion of hand drawings into a subset of \LaTeX . We train the model to generalize to hand drawings by introducing noise into the renderings of the training target images. We designed this noise process to introduce the kinds of variations found in hand drawings (Figure 5; see supplement for details). Our neurally-guided SMC procedure used pixel-wise distance as a surrogate for a likelihood function ($L(\cdot|\cdot)$ in section 3). But pixel-wise distance fares poorly on hand drawings, which never exactly match the model’s renders. So, for hand drawings, we *learn* a surrogate likelihood function, $L_{\text{learned}}(\cdot|\cdot)$. The density $L_{\text{learned}}(\cdot|\cdot)$ is predicted by a convolutional network that we train to predict the distance between two traces

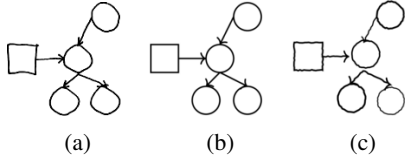


Figure 5: (a): a hand drawing. (b): Rendering of the trace our model infers for (a). We can generalize to hand drawings like these because we train the model on images corrupted by a noise process designed to resemble the kind of noise introduced by hand drawings - see (c) for a noisy rendering of (b).

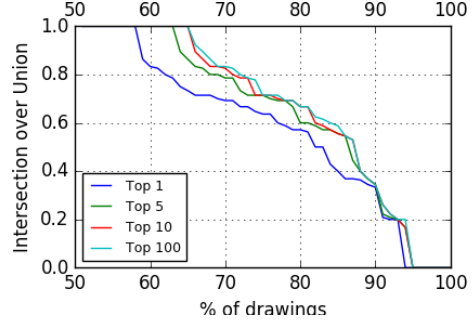


Figure 6: How close are the model’s outputs to the ground truth on hand drawings, as we consider larger sets of samples (1, 5, 10, 100 samples)? Distance to the ground truth trace is measured by the intersection over union of predicted vs. ground truth traces (sets of drawing commands).

conditioned upon their renderings. We train our likelihood surrogate to approximate the symmetric difference, which is the number of drawing commands by which two traces differ:

$$-\log L_{\text{learned}}(\text{render}(T_1)|\text{render}(T_2)) \approx |T_1 - T_2| + |T_2 - T_1| \quad (3)$$

Intuitively, Eq. 3 says that $L_{\text{learned}}(\cdot|\cdot)$ approximates the distance between the trace we want and the trace we have so far. Pixel-wise distance metrics are sensitive to the fine details of how and exactly where arrows, dashes, and corners are drawn – but we wish to be invariant to these details. So, we learn a distance metric over images that approximates the distance metric in the search space over traces.

We drew 100 figures by hand; see figure 7. These were drawn reasonably carefully but not perfectly. Because our model assumes that objects are snapped to a 16×16 grid, we made the drawings on graph paper.

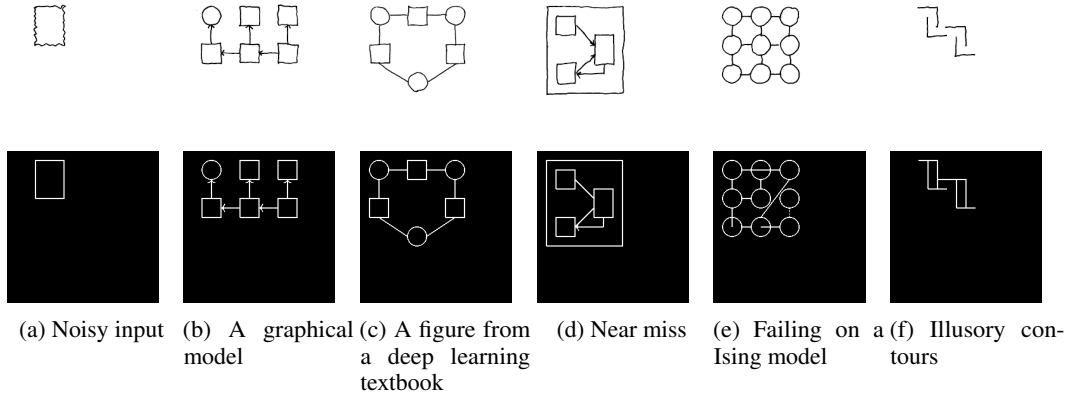


Figure 7: Example drawings above model outputs. See also Fig. 1. Stochastic search (SMC) can help correct for these errors, as can the program synthesizer (Section 4.1)

For each drawing we annotated a ground truth trace, and evaluated the model by asking it to sample many candidate traces for each drawing. For 58% of the drawings the Top-1 most likely sample exactly matches the ground truth; as we consider more samples the model encounters traces that are closer to the ground truth annotation (Fig. 6). Because our current model sometimes makes mistakes on hand drawings, we envision the current system working as follows: a user sketches a diagram, and the system responds by proposing a few candidate interpretations. The user could then select the one closest to their intention and edit it if necessary.

146 4 Synthesizing graphics programs from execution traces

147 Although the execution trace of a graphics program describes the parts of a scene, it fails to encode
 148 higher-level features of the image, such as repeated motifs or symmetries. A *graphics program* better
 149 describe structures like these, and we now take as our goal to synthesize simple graphics programs
 150 from their execution traces.

151 We constrain the space of allowed programs by writing down a context free grammar over a space of
 152 programs. Although it might be desirable to synthesize programs in a Turing-complete language such
 153 as Lisp or Python, a more tractable approach is to specify what in the program languages community
 154 is called a Domain Specific Language (DSL) [12]. Our DSL (Table 2) encodes prior knowledge of
 155 what graphics programs tend to look like.

Program	→	Command; ...; Command
Command	→	circle(Expression, Expression)
Command	→	rectangle(Expression, Expression, Expression, Expression)
Command	→	line(Expression, Expression, Expression, Expression, Boolean, Boolean)
Command	→	for($0 \leq \text{Var} < \text{Expression}$) { if ($\text{Var} > 0$) { Program }; Program }
Command	→	reflect(Axis) { Program }
Expression	→	$\mathcal{Z} * \text{Var} + \mathcal{Z}$
Var	→	A free (unused) variable
\mathcal{Z}	→	an integer
Axis	→	X = \mathcal{Z}
Axis	→	Y = \mathcal{Z}

Table 2: Grammar over graphics programs. We allow loops (for) with conditionals (if), vertical/horizontal reflections (reflect), variables (Var) and affine transformations ($\mathcal{Z} * \text{Var} + \mathcal{Z}$).

156 Given the DSL and a trace T , we want to recover a program that both evaluates to T and, at the same
 157 time, is the “best” explanation of T . For example, we might prefer more general programs or, in the
 158 spirit of Occam’s razor, prefer shorter programs. We wrap these intuitions up into a cost function
 159 over programs, and seek the minimum cost program consistent with T :

$$\text{program}(T) = \arg \min_{\substack{p \in \text{DSL} \\ p \text{ evaluates to } T}} \text{cost}(p) \quad (4)$$

160 We define the cost of a program to be the number of statements it contains, where a statement is a
 161 “Command” in Table 2. We also penalize using many different numerical constants; see supplement.

162 The constrained optimization problem in equation 4 is intractable in general, but there exist efficient-
 163 in-practice tools for finding exact solutions to program synthesis problems like these. We use the
 164 state-of-the-art Sketch tool [1]. Describing Sketch’s program synthesis algorithm is beyond the
 165 scope of this paper; see [1]. At a high level, Sketch takes as input a space of programs, along with
 166 a specification of the program’s behavior and optionally a cost function. It translates the synthesis
 167 problem into a constraint satisfaction problem, and then uses a SAT solver to find a minimum cost
 168 program satisfying the specification. In exchange for not having any guarantees on how long it will
 169 take to find a minimum cost solution, it comes with the guarantee that it will always find a globally
 170 optimal program.

171 Why synthesize a graphics program, if the execution trace already suffices to recover the objects in
 172 an image? Within our domain of hand-drawn figures, graphics program synthesis has several uses:

173 4.1 Correcting errors made by the neural network

174 The program synthesizer can help correct errors from the execution trace proposal network by favoring
 175 execution traces which lead to more concise or general programs. For example, one generally prefers
 176 figures with perfectly aligned objects over figures whose parts are slightly misaligned – and precise
 177 alignment lends itself to short programs. Similarly, figures often have repeated parts, which the
 178 program synthesizer might be able to model as a loop or reflectional symmetry. So, in considering
 179 several candidate traces proposed by the neural network, we might prefer traces whose best programs
 180 have desirable features such as being short or having iterated structures.

181 Concretely, we implemented the following scheme: for an image I , the neurally guided sampling
 182 scheme of section 3 samples a set of candidate traces, written $\mathcal{F}(I)$. Instead of predicting the most
 183 likely trace in $\mathcal{F}(I)$ according to the neural network, we can take into account the programs that best
 184 explain the traces. Writing $\hat{T}(I)$ for the trace the model predicts for image I ,

$$\hat{T}(I) = \arg \max_{T \in \mathcal{F}(I)} L_{\text{learned}}(I|\text{render}(T)) \times \mathbb{P}_{\theta}[T|I] \times \mathbb{P}_{\beta}[\text{program}(T)] \quad (5)$$

185 where $\mathbb{P}_{\beta}[\cdot]$ is a prior probability distribution over programs parameterized by β . This is equivalent
 186 to doing MAP inference in a generative model where the program is first drawn from $\mathbb{P}_{\beta}[\cdot]$, then the
 187 program is executed deterministically, and then we observe a noisy version of the program’s output,
 188 where $L_{\text{learned}}(I|\text{render}(\cdot)) \times \mathbb{P}_{\theta}[\cdot|I]$ is our observation model.

189 Given a corpus of graphics program synthesis problems with annotated ground truth traces (i.e. (I, T)
 190 pairs), we find a maximum likelihood estimate of β :

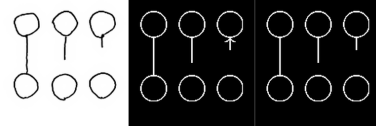
$$\beta^* = \arg \max_{\beta} \mathbb{E} \left[\log \frac{\mathbb{P}_{\beta}[\text{program}(T)] \times L_{\text{learned}}(I|\text{render}(T)) \times \mathbb{P}_{\theta}[T|I]}{\sum_{T' \in \mathcal{F}(I)} \mathbb{P}_{\beta}[\text{program}(T')] \times L_{\text{learned}}(I|\text{render}(T')) \times \mathbb{P}_{\theta}[T'|I]} \right] \quad (6)$$

191 where the expectation is taken both over the model predictions and the (I, T) pairs in the training
 192 corpus. We define $\mathbb{P}_{\beta}[\cdot]$ to be a log linear distribution $\propto \exp(\beta \cdot \phi(\text{program}))$, where $\phi(\cdot)$ is a feature
 193 extractor for programs. We extract a few basic features of a program, such as its size and how many
 194 loops it has, and use these features to help predict whether a trace is the correct explanation for an
 195 image.

196 We synthesized programs for the top five traces output by the deep network. Learning this prior over
 197 programs can help correct mistakes made by the neural network, and also occasionally introduces
 198 mistakes of its own; see Fig. 8 for a representative example of the kinds of corrections that it makes.
 199 On the whole it modestly improves our Top-1 accuracy from 58% to 60%. Recall that from Fig. 6
 200 that the best improvement in accuracy we could possibly get is 63% by looking at the top 5 traces.

201 4.2 Modeling similarity between drawings

202 Modeling an image using a program opens up new ways of
 203 measuring similarity between drawings. For example, we
 204 might say that two drawings are similar if they both contain
 205 repetitions of length 4, or if they share the same reflectional
 206 symmetry, or if they are both organized according to a grid-
 207 like structure.



208 We measure the similarity between two drawings by extract-
 209 ing features of the best programs that describe them. Here
 210 the features we use are just counts of the number of times
 211 that different components in the DSL were used (Table 2).
 212 We project these features down to a 2-dimensional sub-
 213 space using nonnegative matrix factorization (NMF: [13]);
 214 see Fig.9. One could use many alternative similarity met-
 215 rics between drawings which would capture pixel-level or
 216 object-level similarities while missing high-level geomet-
 217 ric similarities. For example, we can use our learned distance metric between execution traces,
 218 $L_{\text{learned}}(\cdot|\cdot)$. Projecting these distances to a 2-dimensional subspace using multidimensional scaling
 219 (MDS: [14]) reveals similarities between the objects in the drawings, while missing similarities at the
 220 level of the program.

Figure 8: Left: hand drawing. Center: interpretation favored by the deep network. Right: interpretation favored after learning a prior over programs. Our learned prior favors shorter, simpler programs, thus continuing the pattern of not having an arrow is preferred.

221 4.3 Extrapolating figures

222 Having access to the source code of a graphics program facilitates coherent, high-level edits to the
 223 figure generated by that program. For example, we can change all of the circles to squares or make all
 224 of the lines be dashed. We can also **extrapolate** figures by increasing the number of times that loops
 225 are executed. Extrapolating repetitive visuals patterns comes naturally to humans, and building this
 226 ability into an application is practical: imagine hand drawing a repetitive graphical model structure
 227 and having our system automatically induce and extend the pattern. Fig. 11 shows extrapolations of
 228 programs synthesized from ground truth traces; see supplement for our full set of extrapolations.



Figure 9: NMF on features of the programs that were synthesized for each image. Horizontal component roughly corresponds to “symmetry” while vertical component roughly corresponds to “loopyness”, with images on the diagonal having both of these.

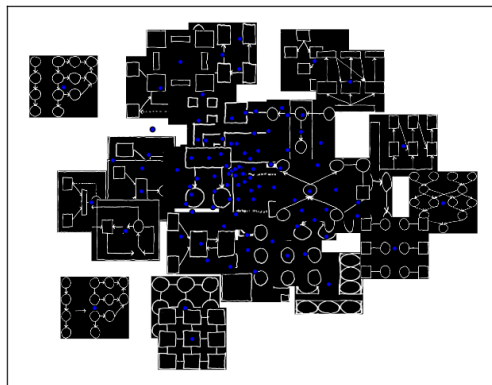


Figure 10: MDS on drawings using the learned distance metric, $L_{\text{learned}}(\cdot|\cdot)$. Drawings with similar looking parts in similar locations are clustered together.

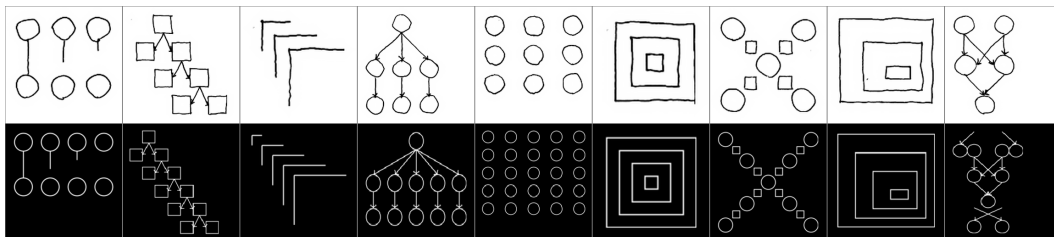


Figure 11: Top: hand drawings. Bottom: extrapolations produced by running loops for extra iterations. Rightmost pair is an illustrative failure case.

5 Conclusion

We have presented a system for inferring graphics programs which generate \LaTeX -style figures from hand-drawn images. The system uses a combination of deep neural networks and stochastic search to parse drawings into symbolic execution traces; it then feeds these traces to a general-purpose program synthesis engine to infer a structured graphics program. We evaluated our model’s performance at parsing novel images, and we demonstrated its ability to extrapolate from provided drawings and to organize them according to high-level geometric features.

There are many directions for future work. In the parsing phase, the proposal network currently samples positional variables on a discrete grid. More general types of drawings could be supported by instead sampling from continuous distributions, e.g. using Mixture Density Networks [15]. The proposal network also currently handles only a very small subset of \LaTeX drawing commands, though there is no reason that it could not be extended to handle more with a higher-capacity network. Exploring more sophisticated network architectures, including ones that utilize attention [16], could also help correct some of the errors the network makes. In the synthesis phase, a more expressive DSL—including subroutines, recursion, and symmetry groups beyond reflections—would allow the system to effectively model a wider variety of graphical phenomena. The synthesizer itself could also be the subject of future work: the system currently uses the general-purpose Sketch synthesizer, which can take minutes to hours to run, whereas program synthesizers which are custom-built for special problem domains can run much faster or even interactively [17].

In the not-too-distant future, we believe it should be possible to produce professional-looking figures just by drawing them and then letting an artificially-intelligent agent write the corresponding code. More generally, we believe that the two-phase system we have proposed—parsing into execution traces, then searching for a low-cost symbolic program which generates those traces—may be a useful

252 paradigm for other domains in which agents must programmatically reason about noisy perceptual
 253 input.

254 References

- 255 [1] Armando Solar Lezama. *Program Synthesis By Sketching*. PhD thesis, EECS Department, University of
 256 California, Berkeley, Dec 2008.
- 257 [2] Leonardo De Moura and Nikolaj Bjørner. Z3: An efficient smt solver. In *Tools and Algorithms for the*
 258 *Construction and Analysis of Systems*, pages 337–340. Springer, 2008.
- 259 [3] SM Eslami, N Heess, and T Weber. Attend, infer, repeat: Fast scene understanding with generative models.
 260 arxiv preprint arxiv:..., 2016. URL <http://arxiv.org/abs/1603.08575>.
- 261 [4] Daniel Ritchie, Anna Thomas, Pat Hanrahan, and Noah Goodman. Neurally-guided procedural models:
 262 Amortized inference for procedural graphics programs using neural networks. In *Advances In Neural*
 263 *Information Processing Systems*, pages 622–630, 2016.
- 264 [5] Haibin Huang, Evangelos Kalogerakis, Ersin Yumer, and Radomir Mech. Shape synthesis from sketches
 265 via procedural models and convolutional networks. *IEEE transactions on visualization and computer*
 266 *graphics*, 2017.
- 267 [6] Gen Nishida, Ignacio Garcia-Dorado, Daniel G. Aliaga, Bedrich Benes, and Adrien Bousseau. Interactive
 268 sketching of urban procedural models. *ACM Trans. Graph.*, 35(4), 2016.
- 269 [7] Brian Hempel and Ravi Chugh. Semi-automated svg programming via direct manipulation. In *Proceedings*
 270 *of the 29th Annual Symposium on User Interface Software and Technology*, UIST '16, pages 379–390,
 271 New York, NY, USA, 2016. ACM.
- 272 [8] Kenneth Forbus, Jeffrey Usher, Andrew Lovett, Kate Lockwood, and Jon Wetzell. Cogsketch: Sketch
 273 understanding for cognitive science research and for education. *Topics in Cognitive Science*, 3(4):648–666,
 274 2011.
- 275 [9] Kevin Ellis, Armando Solar-Lezama, and Josh Tenenbaum. Unsupervised learning by program synthesis.
 276 In *Advances in Neural Information Processing Systems*, pages 973–981, 2015.
- 277 [10] Martín Abadi, Ashish Agarwal, Paul Barham, Eugene Brevdo, Zhifeng Chen, Craig Citro, Greg S. Corrado,
 278 Andy Davis, Jeffrey Dean, Matthieu Devin, Sanjay Ghemawat, Ian Goodfellow, Andrew Harp, Geoffrey
 279 Irving, Michael Isard, Yangqing Jia, Rafal Jozefowicz, Lukasz Kaiser, Manjunath Kudlur, Josh Levenberg,
 280 Dan Mané, Rajat Monga, Sherry Moore, Derek Murray, Chris Olah, Mike Schuster, Jonathon Shlens,
 281 Benoit Steiner, Ilya Sutskever, Kunal Talwar, Paul Tucker, Vincent Vanhoucke, Vijay Vasudevan, Fernanda
 282 Viégas, Oriol Vinyals, Pete Warden, Martin Wattenberg, Martin Wicke, Yuan Yu, and Xiaoqiang Zheng.
 283 TensorFlow: Large-scale machine learning on heterogeneous systems, 2015. Software available from
 284 tensorflow.org.
- 285 [11] Arnaud Doucet, Nando De Freitas, and Neil Gordon, editors. *Sequential Monte Carlo Methods in Practice*.
 286 Springer, 2001.
- 287 [12] Oleksandr Polozov and Sumit Gulwani. Flashmeta: A framework for inductive program synthesis. *ACM*
 288 *SIGPLAN Notices*, 50(10):107–126, 2015.
- 289 [13] Daniel D Lee and H Sebastian Seung. Learning the parts of objects by non-negative matrix factorization.
 290 *Nature*, 401(6755):788–791, 1999.
- 291 [14] Michael AA Cox and Trevor F Cox. Multidimensional scaling. *Handbook of data visualization*, pages
 292 315–347, 2008.
- 293 [15] Christopher M. Bishop. Mixture Density Networks. Technical report, 1994.
- 294 [16] Volodymyr Mnih, Nicolas Heess, Alex Graves, et al. Recurrent models of visual attention. In *Advances in*
 295 *neural information processing systems*, pages 2204–2212, 2014.
- 296 [17] Vu Le and Sumit Gulwani. Flashextract: a framework for data extraction by examples. In *ACM SIGPLAN*
 297 *Notices*, volume 49, pages 542–553. ACM, 2014.